Geometrical phase and Hall effect associated with the transverse spin of light

Meng-Yun Lai,[1,2,*] Yong-Long Wang,[2,4,†] Guo-Hua Liang,[3,‡] and Hong-Shi Zong[1,4,5,§]

[1]*Department of Physics, Nanjing University, Nanjing 210093, China*
[2]*School of Physics and Electronic Engineering, Linyi University, Linyi 276005, China*
[3]*College of Engineering and Applied Sciences, Nanjing University, Nanjing 210093, China*
[4]*Joint Center for Particle and Nuclear Physics and Cosmology, Nanjing 210093, China*
[5]*State Key Laboratory of Theoretical Physics, Institute of Theoretical Physics, CAS, Beijing 100190, China*

(Received 1 March 2019; published 18 September 2019)

By analyzing the vectorial Helmholtz equation within the thin-layer approach, we find that light acquires another geometrical phase, in addition to the usual one (the optical Berry phase), during the propagation along a curved path. Unlike the optical Berry phase, the additional geometrical phase is induced by the curvature of the curve and associated with the transverse spin of light. Furthermore, we show an additional Hall effect of light induced by the torsion of the curve and associated with the transverse spin of light, which is different from the usual spin Hall effect of light. Finally, we demonstrate that the usual and transverse-spin-dependent geometrical phase phenomena are described by different geometry-induced U(1) gauge fields in different adiabatic approximations. In the general case, these gauge fields are united in an effective SO(3) gauge field, and the optical Berry phase and transverse-spin-dependent geometrical phase are united in a general geometrical phase of light.

DOI: 10.1103/PhysRevA.100.033825

I. INTRODUCTION

It has long been known that light carries the spin angular momentum (AM) along the direction of propagation. The longitudinal spin is generated by rotating electric and magnetic fields in the transverse plane. In the past decade, it was shown that light exhibits an unusual transverse spin in various structured optical fields such as evanescent waves, interference fields, and focused beams [1–3]. The transverse spin of light is associated with the presence of a nonvanishing longitudinal component of the electromagnetic field. As early as 1959, Richards and Wolf showed that in an optical focusing system the electromagnetic field oscillates along both transverse and longitudinal directions with $\pi/2$ phase difference [4]. However, they did not identify this elliptical polarization in the propagation plane as the manifestation of nonzero transverse spin of light. Only in 2009 the transverse spin of light and its extraordinary properties, which are very different from those of the longitudinal one, started to attract researchers' interest [5,6]. Most importantly for applications, the transverse spin is locked to the direction of propagation: the sign of the transverse spin AM density flips when the propagation direction reverses [7]. Interestingly, the spin-direction locking in evanescent waves can be recognized as the optical counterpart of the quantum spin Hall effect [8]. Owing to this robust spin-direction locking, the transverse spin AM has found important applications in highly efficient unidirectional optical transport [7,9–15], resulting in a young yet advanced research field: chiral quantum optics [16].

On the other hand, light acquires an optical Berry phase when it propagates along a curved path [17–21]. The optical Berry phase underpins the spin-orbit interactions (SOIs) of light which play a fundamental role in modern optics [22]. The optical Berry phase can be easily understood through the following argument. Consider the three-dimensional vector space attached to each point of a space curve. Due to the vectorial nature of the light field, the three-dimensional vector space relates to the spin space of light propagating along the curve. For a transverse electric field, the three-dimensional vector space reduces to a two-dimensional spin space of light. Consequently, the torsion of the curve, which describes the transport of the spin space along the curve and relates to the connection of the spin space, is coupled with the longitudinal spin and acts as a gauge field within the dynamics along the curve [23]. Then akin to the Aharonov-Bohm phase, this effective gauge field results in the optical Berry phase.

Along these lines it is natural to expect that there are geometrical phase phenomena associated with the transverse spin of light [24], just like with the longitudinal one. In fact, the geometrical quantity of the curve (i.e., the curvature) may be coupled with the spin AM of light. As a consequence, an additional class of geometrical phase phenomena, which are associated with the transverse spin of light, would take place. To study the transverse-spin-dependent geometrical phase phenomena, in Sec. II of this paper we use the thin-layer approach to analyze the vectorial Helmholtz equation and take into consideration the longitudinal component of the electric field at the same time. The thin-layer approach is a convenient framework to study the evolution of various types of waves, including the electromagnetic wave, along a curve or on a curved surface [25–33]. In Sec. III, we discuss the transverse-spin-dependent geometrical phase phenomena. In Sec. IV, we analyze the gauge structure of the present theory. Section V provides conclusions.

*mengyunlai@gmail.com
†wangyonglong@lyu.edu.cn
‡guohua@nju.edu.cn
§zonghs@nju.edu.cn

II. EFFECTIVE EQUATION

The vectorial Helmholtz equation describing the propagation of the electromagnetic wave is obtained from the combination of Maxwell's equations [28,34],

$$\nabla^2\mathbf{E} - \nabla(\nabla\cdot\mathbf{E}) - \frac{n^2}{c^2}\partial_t^2\mathbf{E} = 0. \tag{1}$$

The second term in Eq. (1) leads to a spin and intrinsic orbital AM coupling term for space-varying refractive index (see Ref. [35] and references therein). In the present work, this term is outside the scope of our consideration (see Appendix A). Equation (1) becomes

$$\nabla^2\mathbf{E} - \frac{n^2}{c^2}\partial_t^2\mathbf{E} = 0. \tag{2}$$

According to the well-known result in differential geometry [36], the covariant derivative ∇_i is different from the ordinary derivative $\partial_i = \partial/\partial q^i$ when it acts on a tensor (including vector), where the indices $i, j, \ldots$ run from 1 to 3. For example, when ∇_i acts on a second-order tensor T^{jk}, we have

$$\nabla_i T^{jk} = \partial_i T^{jk} + \Gamma^j_{il}T^{lk} + \Gamma^k_{il}T^{jl}, \tag{3}$$

where Γ^i_{jk} is the Christoffel symbol which relates to the parallel transport of tensors. Apparently, the Christoffel symbols arise in the Laplacian term, $\nabla^2\mathbf{E}$, in the vectorial Helmholtz Eq. (2). By expanding $\nabla^2\mathbf{E}$ in a general curvilinear coordinate system, we obtain

$$\begin{aligned}\nabla^2\mathbf{E} &= \nabla_j\nabla^j E^i \\ &= \frac{1}{\sqrt{g}}\partial_j(\sqrt{g}g^{jk}\partial_k E^i) + 2g^{jk}\Gamma^i_{kl}\partial_j E^l \\ &\quad + \frac{1}{\sqrt{g}}\partial_j(\sqrt{g}g^{jk}\Gamma^i_{kl})E^l + g^{jl}\Gamma^i_{jk}\Gamma^k_{lm}E^m,\end{aligned} \tag{4}$$

where g_{ij} denotes the metric tensor and $g = \det(g_{ij})$. For comparison, the usual Helmholtz equation is

$$\nabla^2 E - \frac{n^2}{c^2}\partial_t^2 E = 0, \tag{5}$$

where $\nabla^2 E = \nabla_i\nabla^i E = 1/\sqrt{g}\partial_j(\sqrt{g}g^{jk}\partial_k E)$ and E denotes the scalar approximation for the electric field. Note that the first term on the right-hand side of Eq. (4) is exactly the Laplacian term in Eq. (5). This term can be expanded as

$$\frac{1}{\sqrt{g}}\partial_j(\sqrt{g}g^{jk}\partial_k E^i) = (\partial_j\partial^j + \Gamma^l_{lj}\partial^j)E^i, \tag{6}$$

where the last term leads to the effective gauge field associated with the intrinsic orbital AM [23,30,37,38]. Unlike this pure orbital term, the last three terms in Eq. (4) only appear in the case of vector waves and, thus, exhibit the vectorial properties of the electromagnetic waves. The second and third terms on the right-hand side of Eq. (4) represent the geometry-induced SOIs of light, since they mix the spin and orbital degrees of freedom by index contraction. The last term in Eq. (4) is a pure spin term; it only relates to the spin degree of freedom. Physically, these geometry-induced terms are associated with the change of the directions of the wave vector and the spin of light. In practice, the variation of the wave vector and the spin directions can be achieved by constructing various optical systems, such as optical fibers [18], two-dimensional curved waveguides [28], gradient-index media [39,40], and plasmonic nanostructures [41,42].

Here, we consider a heuristic model to show how the geometrical quantities influence the propagation of light carrying transverse spin. We focus on the curved propagation of an electromagnetic wave and take into consideration the longitudinal component of the electric field. First of all, let us introduce a coordinate system (we prefer to call it the "adapted coordinate system") [37], in which case the present problem can be simply described. Let $\mathbf{r}_0(s)$ be the parametrization of the curve along which the electromagnetic wave propagates, with s being the arclength. In the vicinity of $\mathbf{r}_0(s)$, the points are described by the following position vector (see Fig. 1):

$$\mathbf{R}(s, q^2, q^3) = \mathbf{r}_0(s) + q^2\mathbf{n}(s) + q^3\mathbf{b}(s), \tag{7}$$

where $\mathbf{n}$ and $\mathbf{b}$ are the unit normal and binormal vectors of $\mathbf{r}_0(s)$, and q^2, q^3 are the corresponding coordinate variables. By introducing the position vector, we define the adapted coordinates system in the vicinity of $\mathbf{r}_0(s)$. The metric tensor in this coordinates system is given by

$$g_{ij} = \partial_i\mathbf{R}\cdot\partial_j\mathbf{R}. \tag{8}$$

Note that the unit tangent, normal, and binormal vectors $\{\mathbf{t} = \partial_s\mathbf{r}_0(s), \mathbf{n}, \mathbf{b}\}$ construct the Frenet frame of $\mathbf{r}_0(s)$. According to the Frenet-Serret formulas, these three vectors and their derivatives with respect to the arclength obey the following equation:

$$\begin{pmatrix}\partial_s\mathbf{t}\\ \partial_s\mathbf{n}\\ \partial_s\mathbf{b}\end{pmatrix} = \begin{pmatrix}0 & \kappa(s) & 0\\ -\kappa(s) & 0 & \tau(s)\\ 0 & -\tau(s) & 0\end{pmatrix}\begin{pmatrix}\mathbf{t}\\ \mathbf{n}\\ \mathbf{b}\end{pmatrix}, \tag{9}$$

where $\kappa(s)$ and $\tau(s)$ are the curvature and torsion of $\mathbf{r}_0(s)$ which describe the rotations of $\mathbf{t}$-$\mathbf{n}$ and $\mathbf{n}$-$\mathbf{b}$ planes along the curve, respectively. Substituting the position vector (7) and Frenet-Serret formulas (9) into the metric (8), we calculate

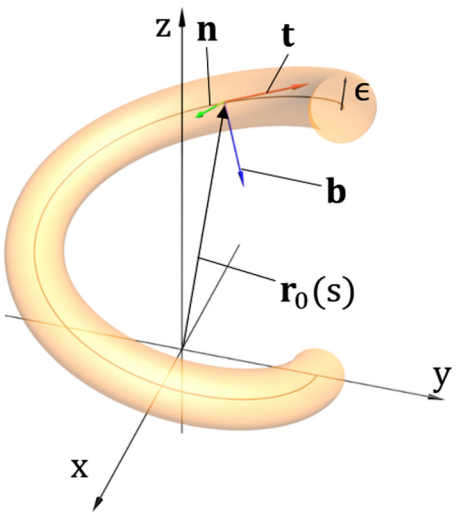

FIG. 1. Schematic of a curved thin tube. $\mathbf{t}$, $\mathbf{n}$, and $\mathbf{b}$ are the unit tangent, normal, and binormal vectors of the curve $\mathbf{r}_0(s)$, respectively. The orange curved tube denotes the vicinity of $\mathbf{r}_0(s)$. ϵ denotes the radius of the normal cross section of the curved tube.

the metric as

$$g_{ij} = \frac{\partial \mathbf{R}}{\partial q^i} \cdot \frac{\partial \mathbf{R}}{\partial q^j} = \begin{pmatrix} g_{11} & -\tau(s)q^3 & \tau(s)q^2 \\ -\tau(s)q^3 & 1 & 0 \\ \tau(s)q^2 & 0 & 1 \end{pmatrix}, \tag{10}$$

where $g_{11} = [1-\kappa(s)q^2]^2 + \tau(s)^2[(q^2)^2 + (q^3)^2]$. By directly calculating with Eq. (10), one can readily obtain nonzero Christoffel symbols and a vanishing Riemannian curvature tensor. This confirms that the adapted coordinate system is just a special curvilinear coordinate system in the three-dimensional Euclidean space.

Now we are able to derive the effective equation that describes the propagation along the curve. First, to get the correct volume measure on $\mathbf{r}_0(s)$, we introduce a new field function $\bar{E}^i = g^{1/4}E^i$ [25,28]. Also, we assume the separation between the tangent and normal parts of the electric field: $\bar{E}^i(s,q^2,q^3) = \bar{E}^i_s(s)\bar{E}_\perp(q^2,q^3)$ [25,28,30,43]. Second, substituting the metric Eq. (10) and the new field function $\bar{E}^i = g^{1/4}E^i$ into the vectorial Helmholtz equation Eq. (2), one can obtain a long equation which consists of q^2, q^3, ∂_i, τ, κ, and $\bar{E}^i$. We emphasize that this long equation is nothing but the vectorial Helmholtz equation written in a special curvilinear coordinate system (the adapted coordinate system). Finally, impose the thin-tube limiting $q^2, q^3 \to 0$ to the long equation. The thin-tube limiting $q^2, q^3 \to 0$ implies the smallness of the scale of the transverse profile of the light beam (i.e., the beamwidth). In practice, the effectiveness of the thin-tube limiting is determined by the parameter $\delta = \max(\epsilon/\tau^{-1}, \epsilon/\kappa^{-1})$, where ϵ is the characteristic beamwidth. Experimentally speaking, the thin-tube limiting can be safely applied to, for example, light propagating in optical fibers and even thin light beams [40]. We emphasize that the above derivations do not depend on the details of how the thin-tube limiting is realized in experiments.

Following the above procedure, we obtain the effective equation describing the propagation along the curve:

$$\left[(\partial_s - i\tau\hat{S}_1 - i\kappa\hat{S}_3)^2 + \frac{\kappa^2}{4} + k_s^2\right]\begin{pmatrix}\bar{E}^1_s(s)\\ \bar{E}^2_s(s)\\ \bar{E}^3_s(s)\end{pmatrix} = 0, \tag{11}$$

where $\hat{S}_1$ and $\hat{S}_3$ are two of the spin-1 matrices,

$$\hat{S}_1 = \begin{pmatrix}0&0&0\\0&0&-i\\0&i&0\end{pmatrix}, \qquad \hat{S}_3 = \begin{pmatrix}0&-i&0\\i&0&0\\0&0&0\end{pmatrix}, \tag{12}$$

and k_s is the wave number. The effective Eq. (11) is the key result in the present paper. It describes the curved propagation of an electromagnetic wave with nonvanishing longitudinal component. Comparing with the trivial one-dimensional wave equation, $(\partial_s^2 + k_s^2)\mathbf{E} = 0$, there are three additional terms appearing in Eq. (11). Unlike the scalar geometrical field $\kappa^2/4$, which results from the action of normal derivatives on the rescale factor [32], the other two additional terms $-i\tau\hat{S}_1$ and $-i\kappa\hat{S}_3$ relate to the parallel transport of the electric field vector along a curve and act as effective gauge terms within the effective dynamics. These two effective gauge terms result in a number of geometry-induced SOIs of light. The torsion-induced one represents the SOI related to the longitudinal spin of light, and thus is responsible for the optical Berry phase and the spin Hall effect associated with the longitudinal spin of light [18,44]. The other term is induced by the curvature, and associated with the transverse spin in the binormal direction. Therefore, we naturally expect that this curvature-induced effective gauge term would lead to transverse-spin-dependent geometrical phase phenomena. In addition, note that expanding $(\partial_s - i\tau\hat{S}_1 - i\kappa\hat{S}_3)^2$ in Eq. (11) would lead to the following term:

$$-\kappa^2\begin{pmatrix}1&0&0\\0&1&0\\0&0&0\end{pmatrix}. \tag{13}$$

This term is responsible for the nonadiabatic polarization changes [21,23]. As we discuss in Sec. IV, according to the spin gauge field theory [45], this term is recognized as the off-diagonal term which is responsible for the transitions between different spin levels of light and can be neglected in the adiabatic approximation. Moreover, the main equations in Refs. [21,23] can be derived from Eq. (11).

III. GEOMETRICAL EFFECTS

The optical Berry phase and the corresponding spin Hall effect have been extensively studied for decades and are thus mostly left out in this paper. In the rest of the present paper, we focus on the curvature-induced effective gauge term and the corresponding geometrical phase phenomena.

A. Transverse-spin-dependent geometrical phase

Without loss of generality, we consider a planar curve here, which means vanishing torsion. The effective Eq. (11) becomes

$$\left[(\partial_s - i\kappa\hat{S}_3)^2 + \frac{\kappa^2}{4} + k_s^2\right]\begin{pmatrix}\bar{E}^1_s(s)\\ \bar{E}^2_s(s)\\ \bar{E}^3_s(s)\end{pmatrix} = 0. \tag{14}$$

Let us diagonalize the above equation by introducing the transverse circular polarizations [11]

$$\begin{pmatrix}\bar{E}^+\\ \bar{E}^-\\ \bar{E}^3\end{pmatrix} = \frac{1}{\sqrt{2}}\begin{pmatrix}1&-i&0\\1&i&0\\0&0&\sqrt{2}\end{pmatrix}\begin{pmatrix}\bar{E}^1\\ \bar{E}^2\\ \bar{E}^3\end{pmatrix}. \tag{15}$$

As the result, Eq. (14) becomes

$$\left[(\partial_s - i\kappa\hat{\sigma})^2 + \frac{\kappa^2}{4} + k_s^2\right]\begin{pmatrix}\bar{E}^+_s\\ \bar{E}^-_s\end{pmatrix} = 0, \tag{16}$$

$$\left(\partial_s^2 + \frac{\kappa^2}{4} + k_s^2\right)\bar{E}^3_s = 0, \tag{17}$$

where $\hat{\sigma} = \left(\begin{smallmatrix}1&0\\0&-1\end{smallmatrix}\right)$. One can readily find that Eq. (16) describes a curvature-induced geometrical phase (transverse-spin-dependent geometrical phase)

$$\Phi_\perp = \sigma_\perp \int \kappa ds, \tag{18}$$

where $\sigma_\perp = \pm 1$ for $\bar{E}^+_s$ and $\bar{E}^-_s$, respectively, and the subscript "$\perp$" indicates that the quantity is associated with the

transverse spin of light. As the torsion-induced geometrical phase $\Phi_{\parallel} = \sigma_{\parallel} \int \tau ds$ induces optical activity in the transverse plane [18], the curvature-induced geometrical phase Eq. (18) leads to an optical rotation in the **t**-**n** plane. Here, $\sigma_{\parallel} = \pm 1$ for left- and right-handed circular polarizations, respectively [22,39], and the subscript "$\parallel$" indicates that the quantity is associated with the longitudinal spin of light. In fact, these two geometrical phases together complete the parallel transport of the electric field with the longitudinal component. Most importantly, the transverse-spin-dependent geometrical phase underpins an additional class of SOI effects of light. Actually, it has already been demonstrated experimentally that the transverse-spin-dependent geometrical phase results in the interaction between the intrinsic orbital AM and the transverse spin of light [24].

So far, we have discussed the transverse-spin-dependent geometrical phase of light from a rather theoretical viewpoint. Next we provide a heuristic but practical example to illustrate the influence of the geometrical phase on the curved propagation of an electromagnetic wave carrying transverse spin. The transverse spin AM of light arises in various structured optical fields such as evanescent waves, interference fields, and focused beams [1–3], due to the strong light confinement [16]. Here, we consider the evanescent wave generated by the total internal reflection at a curved interface between two different media. We assume that the evanescent wave propagates along the curved interface and the total internal reflection is located at $s = 0$. Experimentally speaking, the curved propagation of the evanescent wave may be realized by a whispering-gallery-mode (WGM) microresonator [11,24] or a curved nanophotonic waveguide [12,16]. For a planar interface located at $x = 0$, the evanescent wave propagating along the z direction can be written as [1]

$$\mathbf{E}_p \propto \left(\mathbf{e}_x - i\frac{k_x}{k_z}\mathbf{e}_z\right)e^{ik_z z - k_x x}, \tag{19}$$

where $\mathbf{e}_x$ and $\mathbf{e}_z$ denote the basis vectors of the Cartesian coordinate system, k_z is the wave number, and k_x is the decrement. Then, it would appear reasonable to generalize the evanescent wave (19) to the curved case by demanding the propagation along the curved interface and decay along the perpendicular direction. Thus, the propagation of an evanescent wave along a curve is given by

$$\begin{aligned}\mathbf{E}_c \propto [&(A_+ e^{i\int \kappa ds} + A_- e^{-i\int \kappa ds})\mathbf{t} \\ &+ i(A_+ e^{i\int \kappa ds} - A_- e^{-i\int \kappa ds})\mathbf{n}]e^{ik_s s - k_n q^2},\end{aligned} \tag{20}$$

where the transverse-spin-dependent geometrical phase is included, and A_+ and A_- are the initial amplitudes of the two opposite transverse circular polarizations. The ratio between A_+ and A_- is determined by the initial condition $\mathbf{E}_c(s=0) \propto (\mathbf{n} - ik_n/k_s\mathbf{t})$. Substituting Eq. (20) into the spin AM density [3]

$$\mathbf{S} \propto \mathrm{Im}(\mathbf{E}^* \times \mathbf{E}), \tag{21}$$

one can readily find that the result is exactly the same as the case of planar interface. In other words, the geometrical phase does not change the transverse spin AM density. This suggests the robustness of the spin-direction locking in the case of a curved interface. This trivial result is what we expect, because the transverse-spin-dependent geometrical phase rotates the field vector in the **t**-**n** plane without changing its magnitude. Moreover, as a nontrivial result, one can directly verify that the ratio between the longitudinal and transverse components of the electric field varies periodically along the curved path:

$$\left|\frac{\mathbf{E}_t}{\mathbf{E}_n}\right| = \sqrt{\frac{1 - \left(\frac{n_2}{n_1}\right)^2 \cos^2\left(\int \kappa ds\right)}{1 - \left(\frac{n_2}{n_1}\right)^2 \sin^2\left(\int \kappa ds\right)}}, \tag{22}$$

rather than being a constant: $|\mathbf{E}_t/\mathbf{E}_n| = \sqrt{1-(n_2/n_1)^2}$ [11], where $n_2 > n_1$ are the refractive indices of the different media on each side of the interface. For $n_2/n_1 = 1.4$, Eq. (22) and $\sqrt{1-(n_2/n_1)^2}$ are plotted in Fig. 2(b), where $|\mathbf{E}_t/\mathbf{E}_n|_1$ and $|\mathbf{E}_t/\mathbf{E}_n|_2$ correspond to Eq. (22) and $\sqrt{1-(n_2/n_1)^2}$, respectively.

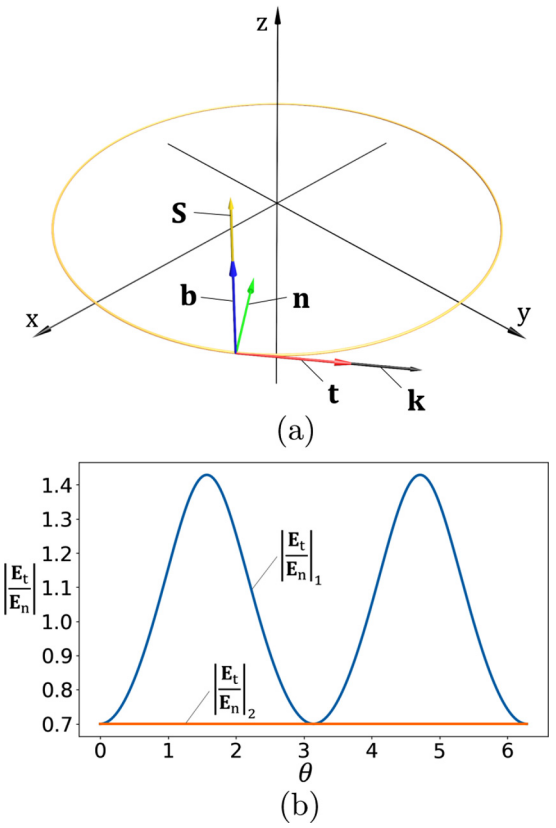

FIG. 2. (a) Schematic of a planar curve. Light propagates along the tangent direction and the transverse spin AM is along the binormal direction. Although we plot a circle here, Eqs. (16) and (18) can be applied to general planar geometries. (b) The ratio between the longitudinal and transverse components of the electric field varies as the function of θ, where $\theta = \int \kappa ds$.

B. Transverse-spin-dependent Hall effect

Alternatively, the transverse-spin-dependent geometrical phase phenomena can be described by a more abstract and general formalism, that is, the Berry connection within the Berry phase formalism. As in the situation of the optical Berry phase $\Phi_{\parallel} = \sigma_{\parallel} \int \tau ds$, the Berry connection $\mathbf{A}_{\perp}$ and the corresponding Berry curvature $\mathbf{F}_{\perp}$ associated with the

transverse spin are defined by [46]

$$\mathbf{A}_\perp(\mathbf{k}) = \mathbf{n}\cdot(\nabla_\mathbf{k})\mathbf{t}, \qquad \mathbf{F}_\perp(\mathbf{k}) = \nabla_\mathbf{k}\times\mathbf{A}_\perp. \tag{23}$$

Importantly, these two geometrical quantities act as an effective vector field and magnetic field in the $\mathbf{k}$ space, with $\sigma_\perp$ in Eq. (18) playing the role of effective charge. By introducing the Berry phase formalism, we can calculate the geometrical phase Eq. (18) through the Berry connection in the $\mathbf{k}$ space:

$$\Phi_\perp = \sigma_\perp\int_C \mathbf{A}_\perp\cdot d\mathbf{k}, \tag{24}$$

where C is the contour of the evolution of $\mathbf{b}$ in the $\mathbf{k}$ space. In particular, for a closed contour the curvature-induced geometrical phase is determined by the solid angle enclosed by the contour.

Let us consider the propagation during one period of a uniform helix as a simple example [see Fig. 3(a)]. The Berry connection and Berry curvature for such propagation can be easily obtained in spherical coordinates (k,θ,ϕ):

$$\mathbf{A}_\perp(\mathbf{k}) = \frac{1}{k}(0,0,1), \qquad \mathbf{F}_\perp(\mathbf{k}) = \frac{1}{k^2}(\cot\Theta,0,0). \tag{25}$$

After the propagation, the transverse-spin-dependent geometrical phase can be calculated by Eq. (18) or (24). The final result is

$$\Phi_\perp = \sigma_\perp 2\pi\sin\Theta, \tag{26}$$

where Θ is the angle between the tangent vector and z axis. Alternatively, one can determine this geometrical phase by calculating the solid angle subtended by the trajectory of $\mathbf{b}$ [see Fig. 3(b)],

$$\begin{aligned}\Phi_\perp^B &= -\sigma_\perp\Omega_\perp(C) = -\sigma_\perp\int_0^{2\pi}\int_{\pi/2+\Theta}^{\pi}\sin\theta d\theta d\phi\\ &= \sigma_\perp 2\pi(\sin\Theta-1),\end{aligned} \tag{27}$$

where $\Omega_\perp(C)$ is the solid angle enclosed by the contour C. Equation (27) coincides with Eq. (26) up to the $-\sigma_\perp 2\pi$ difference caused by the rotation of the ϕ coordinates [22,39]. Passingly, the intriguing equivalence relation between the integration $\int\kappa ds$ and the solid angle $\Omega_\perp(C)$ can be alternatively demonstrated by referring to the argument provided in Ref. [20] by Haldane.

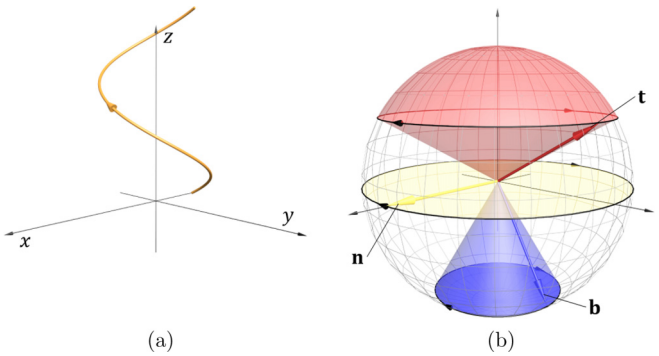

(a) (b)

FIG. 3. (a) One period of a uniform helix with the pitch angle Θ. (b) The rotations of the Frenet frame and the corresponding solid angles during the propagation along the helix.

As we know, the geometrical phase and the spin Hall effect are two reciprocal phenomena [39]. For example, the spin Hall effect of light, which is associated with the optical Berry phase $\Phi_\parallel = \sigma_\parallel\int\tau ds$, is described by [39]

$$\delta\dot{\mathbf{r}}_\parallel = -\sigma_\parallel k_0^{-1}\dot{\mathbf{k}}\times\mathbf{F}_\parallel = -\sigma_\parallel k^{-1}\kappa\mathbf{b}, \tag{28}$$

where $\mathbf{F}_\parallel$ is the effective magnetic field associated with the longitudinal spin of light. Thus, one can readily obtain a similar expression for the spin Hall effect associated with the transverse-spin-dependent geometrical phase (18) by replacing the longitudinal quantities with transverse ones in the above equation. The result is

$$\delta\dot{\mathbf{r}}_\perp = -\sigma_\perp k_0^{-1}\dot{\mathbf{k}}\times\mathbf{F}_\perp = \sigma_\perp k^{-1}\tau\mathbf{b}. \tag{29}$$

This quantity represents the transverse deflection of a light beam propagation along a curved path due to the presence of the transverse spin of light. This transverse-spin-dependent Hall effect is of the same magnitude comparing with the longitudinal one, and thus can be observed through optical experiments. In fact, the usual and transverse-spin-dependent geometrical phase phenomena correspond to different adiabatic approximations. Mathematically, the difference relates to which spin-1 matrix in Eq. (11) is diagonalized, and the terminology "adiabatic" indicates rejecting the off-diagonal terms in Eq. (11) after the diagonalization [45]. Physically, the difference and "adiabatic" relate to the adiabatic transports of the circular polarizations or transverse circular polarizations. As we show in Sec. IV, in the proper adiabatic approximation, the evolution of light can be adequately described by a U(1) gauge field. As a result, Eqs. (28) and (29) are valid in different adiabatic approximations in terms of the Berry phase formalism. In conclusion, when transverse circular polarizations adiabatically transport along a curved path with nonvanishing torsion, a transverse-spin-dependent transverse deflection of the light beam occurs. This is the transverse-spin-dependent Hall effect of light. To observe this effect in the laboratory, the following two requirements are necessary: (1) the adiabatic transport of the transverse spin during the propagation along a curved path, and (2) nonvanishing torsion of the curved path. Requirement 1 is to guarantee the validity of the spin gauge theory [45], while 2 is to guarantee that the transverse-spin-dependent deflection $\delta\dot{\mathbf{r}}_\perp$ is nonzero.

IV. GAUGE STRUCTURE

Within the Berry phase formalism, the usual and transverse-spin-dependent geometrical phase phenomena are associated with different three-dimensional U(1) gauge fields: $\mathbf{A}_\parallel(\mathbf{k}) = \mathbf{b}\cdot(\nabla_\mathbf{k})\mathbf{n}$ and $\mathbf{A}_\perp(\mathbf{k}) = \mathbf{n}\cdot(\nabla_\mathbf{k})\mathbf{t}$ [see Ref. [39] and Eq. (23)]. These two different U(1) gauge fields in the momentum space correspond to the torsion and curvature of the curve, respectively. As shown in Eq. (11), they are united in one wave equation.

Here, we discuss the effective gauge terms in Eq. (11) from the point of view of the gauge theory, and show that they can be unified into an effective SO(3) gauge field. Consider an arbitrary curve in general electromagnetic field. For the sake of generality, we replace the Frenet frame $\{\mathbf{t},\mathbf{n},\mathbf{b}\}$ with an arbitrary triad $\{\mathbf{q}_i(s)\}$. The angular velocity matrices that describe the rotations of the triad along the curve are defined

as follows:

$$\Omega_{ij} = \mathbf{q}_i \cdot \partial_s \mathbf{q}_j, \tag{30}$$

where $\{\mathbf{q}_i(s)\}$ are the three bases of the triad. Consequently, the angular velocity vector is defined in terms of these matrices as

$$\Omega_i = -\tfrac{1}{2}\epsilon_{ijk}\Omega_{jk}, \tag{31}$$

where ϵ_{ijk} is the three-dimensional Levi-Civita symbol. As an example, the angular velocity vector of the Frenet frame is

$$\mathbf{\Omega}_F = \tau\mathbf{t} + \kappa\mathbf{b}. \tag{32}$$

Consider an arbitrary local rotation for the triad $\{\mathbf{q}_i\}$, which is represented by the local rotation angle $\boldsymbol{\theta}(s)$. The local rotation is given by

$$\mathbf{q}_i \to (e^{i\hat{\mathbf{S}}\cdot\boldsymbol{\theta}(s)})_{ij}\mathbf{q}_j. \tag{33}$$

As the result, the angular velocity matrix transforms as an SO(3) gauge connection

$$\begin{aligned}\Omega_{ij} &\to [(e^{i\hat{\mathbf{S}}\cdot\boldsymbol{\theta}})_{ik}\mathbf{q}_k]\partial_s[(e^{i\hat{\mathbf{S}}\cdot\boldsymbol{\theta}})_{jl}\mathbf{q}_l] \\ &= (e^{i\hat{\mathbf{S}}\cdot\boldsymbol{\theta}})_{ik}\Omega_{kl}(e^{i\hat{\mathbf{S}}\cdot\boldsymbol{\theta}})_{jl} + (e^{i\hat{\mathbf{S}}\cdot\boldsymbol{\theta}})_{ik}\partial_s(e^{i\hat{\mathbf{S}}\cdot\boldsymbol{\theta}})_{jk}.\end{aligned} \tag{34}$$

Under the SO(3) rotation (33), the transformation for the electric field components corresponding to the triad is

$$E_i \to (e^{i\hat{\mathbf{S}}\cdot\boldsymbol{\theta}(s)})_{ij}E_j. \tag{35}$$

In terms of Eqs. (34) and (35) and note that $(\hat{S}_i)_{jk} = -i\epsilon_{ijk}$, it can be easily verified that

$$\begin{aligned}&\partial_s E_l - i\Omega_i(\hat{S}_i)_{lm}E_m \to \\ &\quad (e^{i\hat{\mathbf{S}}\cdot\boldsymbol{\theta}(s)})_{lm}[\partial_s E_m - i\Omega_i(\hat{S}_i)_{mn}E_n].\end{aligned} \tag{36}$$

Equations (34), (35), and (36) suggest the minimal coupling between the electric field and the SO(3) gauge connection,

$$\partial_s E_l \to \partial_s E_l - i\Omega_i(\hat{S}_i)_{lm}E_m, \tag{37}$$

which explains the appearance of the effective gauge terms in the effective Eq. (11) from the view of the gauge theory.

With the minimal coupling (37), one can readily find that the general form of the effective equation describing the propagation of light along a curve is

$$\left[(\partial_s - i\mathbf{\Omega}\cdot\hat{\mathbf{S}})^2 + k^2\right]\begin{pmatrix}E^1\\E^2\\E^3\end{pmatrix} = 0. \tag{38}$$

By acting the row vector (E^{1*}, E^{2*}, E^{3*}) on the left of Eq. (38), we can solve it approximately and obtain the general geometrical phase of light

$$\Phi_g = \int \mathbf{S}\cdot\mathbf{\Omega}ds, \tag{39}$$

where the asterisk denotes complex conjugate, and $\mathbf{S} = |\mathbf{E}|^{-2}\mathrm{Im}(\mathbf{E}^*\times\mathbf{E})$ is the spin angular momentum density. Within the Frenet frame, the general geometrical phase of light reduces to the optical Berry phase and the transverse-spin-dependent geometrical phase. By replacing the triad $\{\mathbf{q}_i(s)\}$ with $\{\mathbf{a},\mathbf{b},\mathbf{s}\}$, Eq. (39) becomes the so-called geometric-Coriolis-Doppler phase shift [47], where $\mathbf{a}$ and $\mathbf{b}$ are the unit vectors along the major and minor semiaxes of the polarization ellipse, respectively, and $\mathbf{s} = \mathbf{S}/|\mathbf{S}|$. Therefore, within the triad $\{\mathbf{a},\mathbf{b},\mathbf{s}\}$, Eq. (39) can describe the Pancharatnam-Berry phase, including its transverse-spin-dependent version.

In the spirit of the spin gauge field theory [45], a U(1) gauge field arises in the adiabatic approximation [23]. The adiabatic approximation is associated with the diagonalizations of the three spin-1 matrices. Here, we take the diagonalization of $\hat{S}_3$ as an example (the case of $\hat{S}_1$ is presented in Ref. [23]). The diagonalization can be achieved by the transformation (15). After the diagonalization, neglecting the off-diagonal terms leads to the reduction of Eq. (11) to Eq. (16). Apparently, neglecting the off-diagonal terms corresponds to the adiabatic transports of the transverse circular polarizations. In this adiabatic approximation, the local rotation (33) reduces to an SO(2) rotation

$$\begin{pmatrix}\mathbf{q}_1\\\mathbf{q}_2\end{pmatrix} \to e^{i\hat{\sigma}_s\theta(s)}\begin{pmatrix}\mathbf{q}_1\\\mathbf{q}_2\end{pmatrix}, \tag{40}$$

where $\hat{\sigma}_s = \left(\begin{smallmatrix}0 & -i\\ i & 0\end{smallmatrix}\right)$. For simplicity, here we have neglected the trivial dimension $\mathbf{q}_3$. The transformations for the corresponding SO(2) gauge connection and the electric field become

$$\Omega_3 \to \Omega_3 + \partial_s\theta \tag{41}$$

and

$$E^{\sigma_\perp} \to e^{i\sigma_\perp\theta(s)}E^{\sigma_\perp}, \tag{42}$$

respectively, where $E^{\sigma_\perp}$ denote the two opposite transverse circular polarizations [see Eq. (15)]. Consequently, an effective one-dimensional U(1) gauge field [note that the SO(2) group is isomorphic to the U(1) group] arises in the coordinate space. Within the Berry phase formalism, it corresponds to the three-dimensional U(1) gauge field, $\mathbf{A}_\perp(\mathbf{k})$, in the momentum space.

V. CONCLUSIONS

In the present paper, we investigate the effective dynamics of light with nonvanishing longitudinal component by using the thin-layer approach. As the result, we obtain an effective equation (11) which describes the curved propagation of light exhibiting the longitudinal component. In addition to the torsion-induced term [23], Eq. (11) contains a curvature-induced effective gauge term. This curvature-induced effective gauge term brings about an additional geometrical phase which is associated with the transverse spin along the binormal direction. Furthermore, we show that the curvature-induced effective gauge term is responsible for the nonadiabatic polarization changes of light [21,23]. Imitating the reciprocal relation between the optical Berry phase and the spin Hall effect of light, we calculate the transverse-spin-dependent Hall effect of light. In contrast to the spin Hall effect of light [44], this additional Hall effect induced by the torsion is associated with the transverse spin along the binormal direction of the curve. Interestingly, we find that the usual (longitudinal-spin-dependent) and the additional (transverse-spin-dependent) geometrical phase phenomena are associated

with different geometry-induced U(1) gauge fields in different adiabatic approximations. We demonstrate that these U(1) gauge fields are unified into an effective SO(3) gauge field, and obtain a general geometrical phase of light. The general geometrical phase is able to represent a broad range of optical geometrical phase phenomena, including the usual optical Berry phase, the usual Pancharatnam-Berry phase, and their transverse-spin-dependent versions.

As discussed, the transverse-spin-dependent geometrical phase effects have purely geometrical origin like the longitudinal-spin-dependent ones. It therefore provides new possibilities to control the spin and orbital degrees of freedom of light via the geometries. As an experimental example, the transverse-spin-dependent geometrical phase can be employed to investigate the interaction between the transverse spin and the intrinsic orbital AM of light [24]. We believe that the present research could benefit the rapidly growing research of the transverse spin of light.

ACKNOWLEDGMENTS

We thank Prof. F. Wang for very helpful discussions about gauge theory. This work was supported in part by the National Natural Science Foundation of China (under Grants No. 11690030, No. 11535005, No. 11625418, and No. 51721001) and the Fundamental Research Funds for the Central Universities (under Grant No. 020414380074). Y.-L.W. was funded by the Natural Science Foundation of Shandong Province of China (Grant No. ZR2017MA010) and Linyi University (Grant No. LYDX2016BS135).

APPENDIX A: DISCUSSION OF THE TERM $-\nabla(\nabla\cdot\mathbf{E})$

The Maxwell's equations are

$$\nabla\times\mathbf{E}=-\frac{1}{c}\partial_t\mathbf{B}, \tag{A1}$$

$$\nabla\times\mathbf{H}=\frac{1}{c}\partial_t\mathbf{D}, \tag{A2}$$

$$\nabla\cdot\mathbf{D}=0, \tag{A3}$$

$$\nabla\cdot\mathbf{B}=0. \tag{A4}$$

From Eqs. (A1) and (A2) and the constitutive relations, we can obtain the following vectorial Helmholtz equation:

$$\nabla^2\mathbf{E}-\nabla(\nabla\cdot\mathbf{E})-\frac{n^2}{c^2}\partial_t^2\mathbf{E}=0, \tag{A5}$$

where the second term $-\nabla(\nabla\cdot\mathbf{E})$ survived in the above equation for space-varying refractive index because of Eq. (A3). In our model the refractive index depends only on the perpendicular distance ρ from the curve [21] [i.e., $n=n(\rho)$], where $\{\rho=\sqrt{(q_2)^2+(q_3)^2},\phi=\tan(q_3/q_2)\}$ are the polar coordinates of the transverse plane. In fact, the refractive index of our model can be described by the following function which contains a Heaviside step function (see Ref. [35] and references therein):

$$n(\rho)=n_{\text{core}}+H(a-\rho)\Delta n, \tag{A6}$$

where $H(a-\rho)$ is the Heaviside step function, a is the fiber radius, $\Delta n=n_{\text{core}}-n_{\text{clad}}$, and n_{core} and n_{clad} are the indices of the core and the cladding, respectively. For $\rho<a$ (i.e., in the core of the fiber), we have $n(\rho)=n_{\text{core}}=$ constant, as the result the term $-\nabla(\nabla\cdot\mathbf{E})$ vanishes. According to the theory of Ref. [35] (and references therein), if we take the step profile of the refractive index into consideration, the term $-\nabla(\nabla\cdot\mathbf{E})$ leads to a SOC (spin and intrinsic orbital AM coupling) correction term. The SOC correction term is

$$\hat{H}_{\text{SOC}}=\frac{\delta(\rho-a)\Delta}{4k_z a^2}\left(\frac{1}{a}\partial_\rho-\frac{a}{\rho}\hat{s}_z\hat{l}_\phi\right), \tag{A7}$$

where $\delta(\rho-a)$ is the Dirac delta function and comes from the derivative of $H(a-\rho)$, $\Delta=n_{\text{core}}^2-n_{\text{clad}}^2$ is the dielectric jump at $\rho=a$, k_z is a variable separation constant, and $\hat{s}_z$ and $\hat{l}_\phi=-i\partial_\phi$ are the spin and intrinsic orbital AM operators, respectively.

$\hat{H}_{\text{SOC}}$ is added as a perturbation. Up to the first order, perturbations to k_z can be obtained by calculating the expectation value of $\hat{H}_{\text{SOC}}$:

$$\delta k_z^\sigma=\frac{\pi\Delta}{2k_z a^3}\int\delta(\rho-a)E_\sigma\left(\rho\frac{\partial}{\partial\rho}-\sigma m\right)E_\sigma d\rho, \tag{A8}$$

where $\sigma=\pm1$ is the helicity and m is the eigenvalue of the intrinsic orbital AM (i.e., the vortex number) [35]. Since the perturbation δk_z^σ contains the term σm, it leads to a splitting between the σ_+ and σ_- components. This effect has been observed in experiments as the rotation of the spatial intensity pattern given by the interference of two beams with opposite intrinsic orbital AM [35,48]. When $\Delta=1.12$, the absolute value of δk_z^σ is about 0.1% of the original eigenvalue k_z^0 [35]. For a fiber, Δ is typically about 0.01; then the absolute value of δk_z^σ is about 0.001% of the original eigenvalue k_z^0.

More importantly, the SOC correction term arises in the transverse effective equation rather than the tangent effective equation since it contains only the transverse variables. In our paper, we only focus on the tangent dynamics of light, i.e., the propagation along the curve. Therefore, the effects resulting from $-\nabla(\nabla\cdot\mathbf{E})$ do not change the main results of the present paper. Furthermore, in the present paper, we do not consider the intrinsic orbital AM of light. That is, in our paper light does not carry the intrinsic orbital AM, which means that the spin and intrinsic orbital AM coupling resulting from the term $-\nabla(\nabla\cdot\mathbf{E})$ vanishes. Actually, in the paper the only spin-orbit coupling is the spin and extrinsic orbital AM coupling which leads to the geometrical phase phenomena. We can say that the term $-\nabla(\nabla\cdot\mathbf{E})$ is outside the scope of our consideration in the present paper.

So in conclusion, the term $-\nabla(\nabla\cdot\mathbf{E})$ can be safely ignored in our paper. Equation (A5) becomes

$$\nabla^2\mathbf{E}-\frac{n^2}{c^2}\partial_t^2\mathbf{E}=0. \tag{A9}$$

APPENDIX B: FROM THE POINT OF VIEW OF THE CORIOLIS EFFECT

As discussed above, the geometrical phases of light are straightforward consequences of the Maxwell's equations, and are associated with the parallel transport of the electric field vector. Alternatively, they can be derived through a different way. Note that an arbitrary rotation with respect to a laboratory coordinate frame is described by a precession of the triad

attached to the curve with the angular velocity vector (31) [39]. Analogously to the Coriolis effect in classical mechanics [49], some inertia terms arise in the Helmholtz equation via the following substitution [39,50]:

$$\partial_t \mathbf{E} \to \partial_t \mathbf{E} + \frac{c}{n}\mathbf{\Omega} \times \mathbf{E}, \tag{B1}$$

where the angular-velocity-induced term is the Coriolis term in this situation. Since the time t is associated with the arclength s by the wave velocity c/n, the Coriolis term can be alternatively introduced through the following way:

$$\begin{aligned}\partial_s \mathbf{E} &= \partial_s (E_t \mathbf{t} + E_n \mathbf{n} + E_b \mathbf{b}) \\ &= (\partial_s E_t)\mathbf{t} + (\partial_s E_n)\mathbf{n} + (\partial_s E_b)\mathbf{b} + \mathbf{\Omega} \times \mathbf{E}. \end{aligned} \tag{B2}$$

Importantly, the last row in the above equation can be rewritten in the following form:

$$(\partial_s - i\mathbf{\Omega} \cdot \hat{\mathbf{S}}) \begin{pmatrix} E_t \\ E_n \\ E_b \end{pmatrix}, \tag{B3}$$

which coincides with Eq. (11). Note that we have used a special triad—the Frenet frame—rather than an arbitrary triad in the above derivations. In the Frenet frame, the rotation of the **b**-**t** plane vanishes, and thus the second spin-1 matrix $\hat{S}_2$ does not appear in Eq. (11). In conclusion, we have demonstrated the equivalence between the effective gauge terms in Eq. (11) and the Coriolis terms here. It is obvious that the derivation of the Coriolis terms is much simpler. Nevertheless, like the Coriolis effect in classical mechanics, the introduction of the Coriolis terms here is somewhat artificial. Most importantly, the Coriolis terms are irrelevant to the spatial distribution of the electric field, which means that they cannot describe the geometrical phase phenomena associated with the intrinsic orbital AM. On the other hand, as we have shown in Ref. [23], the orbital geometrical phase can also be directly derived from the Maxwell's equations by using the same approach presented in Sec. II. Physically speaking, once we replace the ordinary differential with the covariant differential, the parallel transport of the electric field is included in the Maxwell's equations. In particular, the parallel transport of the vortex is also included as the polarization.

[1] K. Y. Bliokh, A. Y. Bekshaev, and F. Nori, Nat. Commun. **5**, 3300 (2014).
[2] A. Aiello, P. Banzer, M. Neugebauer, and G. Leuchs, Nat. Photonics **9**, 789 (2015).
[3] K. Y. Bliokh and F. Nori, Phys. Rep. **592**, 1 (2015).
[4] B. Richards, E. Wolf, and G. Dennis, Proc. R. Soc. London A **253**, 358 (1959).
[5] A. Aiello, N. Lindlein, C. Marquardt, and G. Leuchs, Phys. Rev. Lett. **103**, 100401 (2009).
[6] A. Aiello, C. Marquardt, and G. Leuchs, Phys. Rev. A **81**, 053838 (2010).
[7] L. Marrucci, Nat. Phys. **11**, 9 (2014).
[8] K. Y. Bliokh, D. Smirnova, and F. Nori, Science **348**, 1448 (2015).
[9] F. J. Rodríguez-Fortuño, G. Marino, P. Ginzburg, D. O'Connor, A. Martínez, G. A. Wurtz, and A. V. Zayats, Science **340**, 328 (2013).
[10] A. E. Miroshnichenko and Y. S. Kivshar, Science **340**, 283 (2013).
[11] C. Junge, D. O'Shea, J. Volz, and A. Rauschenbeutel, Phys. Rev. Lett. **110**, 213604 (2013).
[12] J. Petersen, J. Volz, and A. Rauschenbeutel, Science **346**, 67 (2014).
[13] R. Mitsch, C. Sayrin, B. Albrecht, P. Schneeweiss, and A. Rauschenbeutel, Nat. Commun. **5**, 5713 (2014).
[14] D. O'Connor, P. Ginzburg, F. J. Rodríguez-Fortuño, G. A. Wurtz, and A. V. Zayats, Nat. Commun. **5**, 5327 (2014).
[15] H. Pichler, T. Ramos, A. J. Daley, and P. Zoller, Phys. Rev. A **91**, 042116 (2015).
[16] P. Lodahl, S. Mahmoodian, S. Stobbe, A. Rauschenbeutel, P. Schneeweiss, J. Volz, H. Pichler, and P. Zoller, Nature (London) **541**, 473 (2017).
[17] J. N. Ross, Opt. Quantum Electron. **16**, 455 (1984).
[18] R. Y. Chiao and Y.-S. Wu, Phys. Rev. Lett. **57**, 933 (1986).
[19] A. Tomita and R. Y. Chiao, Phys. Rev. Lett. **57**, 937 (1986).
[20] F. D. M. Haldane, Opt. Lett. **11**, 730 (1986).
[21] M. Berry, Nature (London) **326**, 277 (1987).
[22] K. Y. Bliokh, F. J. Rodriguez-Fortuno, F. Nori, and A. V. Zayats, Nat. Photonics **9**, 796 (2015).
[23] M.-Y. Lai, Y.-L. Wang, G.-H. Liang, F. Wang, and H.-S. Zong, Phys. Rev. A **97**, 033843 (2018).
[24] Z. Shao, J. Zhu, Y. Chen, Y. Zhang, and S. Yu, Nat. Commun. **9**, 926 (2018).
[25] R. C. T. da Costa, Phys. Rev. A **23**, 1982 (1981).
[26] M. Burgess and B. Jensen, Phys. Rev. A **48**, 1861 (1993).
[27] P. Ouyang, V. Mohta, and R. Jaffe, Ann. Phys. **275**, 297 (1999).
[28] S. Batz and U. Peschel, Phys. Rev. A **78**, 043821 (2008).
[29] V. H. Schultheiss, S. Batz, A. Szameit, F. Dreisow, S. Nolte, A. Tünnermann, S. Longhi, and U. Peschel, Phys. Rev. Lett. **105**, 143901 (2010).
[30] H. Taira, J. Phys. B: At., Mol. Opt. Phys. **44**, 195401 (2011).
[31] Y.-L. Wang, L. Du, C.-T. Xu, X.-J. Liu, and H.-S. Zong, Phys. Rev. A **90**, 042117 (2014).
[32] Y.-L. Wang, H. Jiang, and H.-S. Zong, Phys. Rev. A **96**, 022116 (2017).
[33] G.-H. Liang, Y.-L. Wang, M.-Y. Lai, H. Liu, H.-S. Zong, and S.-N. Zhu, Phys. Rev. A **98**, 062112 (2018).
[34] L. D. Landau, E. M. Lifshitz, and L. P. Pitaevskii, *The Classical Theory of Fields* (Butterworth-Heinemann, Oxford, 1980).
[35] G. Li, A. S. Sheremet, R. Ge, T. C. H. Liew, and A. V. Kavokin, Phys. Rev. Lett. **121**, 053901 (2018).
[36] M. Nakahara, *Geometry, Topology and Physics*, 2nd ed. (IOP Publishing, Bristol, 2003).
[37] P. Schuster and R. Jaffe, Ann. Phys. **307**, 132 (2003).
[38] Y.-L. Wang, M.-Y. Lai, F. Wang, H.-S. Zong, and Y.-F. Chen, Phys. Rev. A **97**, 042108 (2018).
[39] K. Y. Bliokh, J. Opt. A: Pure Appl. Opt. **11**, 094009 (2009).
[40] K. Y. Bliokh and A. S. Desyatnikov, Phys. Rev. A **79**, 011807(R) (2009).
[41] D. Haefner, S. Sukhov, and A. Dogariu, Phys. Rev. Lett. **102**, 123903 (2009).

[42] D. Pan, H. Wei, L. Gao, and H. Xu, Phys. Rev. Lett. **117**, 166803 (2016).
[43] S. Longhi, Opt. Lett. **32**, 2647 (2007).
[44] K. Y. Bliokh, A. Niv, V. Kleiner, and E. Hasman, Nat. Photonics **2**, 748 (2008).
[45] K. Bliokh and Y. Bliokh, Ann. Phys. **319**, 13 (2005).
[46] K. Y. Bliokh, Y. Gorodetski, V. Kleiner, and E. Hasman, Phys. Rev. Lett. **101**, 030404 (2008).
[47] K. Y. Bliokh, M. A. Alonso, and M. R. Dennis, arXiv:1903.01304v2.
[48] D. L. P. Vitullo, C. C. Leary, P. Gregg, R. A. Smith, D. V. Reddy, S. Ramachandran, and M. G. Raymer, Phys. Rev. Lett. **118**, 083601 (2017).
[49] H. Goldstein, C. P. Poole, and J. Safko, *Classical Mechanics* (Pearson Education Limited, Harlow, 2014).
[50] S. G. Lipson, Opt. Lett. **15**, 154 (1990).